STEM CELLS AND DEVELOPMENT
Volume 33, Numbers 13–14, 2024

DOI: 10.1089/scd.2023.0295

Lysyl Oxidase Production by Murine C3H10T1/2 Mesenchymal Stem Cells Is Increased by TGFβs and Differentially Modulated by Mechanical Stimuli

Nicholas M. Pancheri,[1] Allison J. Ellingson,[1] Colin R. Marchus,[1] Vibhav Durgesh,[2] Tabitha Verhage,[1] Nicholas Yensen,[1] and Nathan R. Schiele[1]

Tendons are frequently injured and have limited regenerative capacity. This motivates tissue engineering efforts aimed at restoring tendon function through strategies to direct functional tendon formation. Generation of a crosslinked collagen matrix is paramount to forming mechanically functional tendon. However, it is unknown how lysyl oxidase (LOX), the primary mediator of enzymatic collagen crosslinking, is regulated by stem cells. This study investigates how multiple factors previously identified to promote tendon formation and healing (transforming growth factor [TGF]β1 and TGFβ2, mechanical stimuli, and hypoxia-inducible factor [HIF]-1α) regulate LOX production in the murine C3H10T1/2 mesenchymal stem cell (MSC) line. We hypothesized that TGFβ signaling promotes LOX activity in C3H10T1/2 MSCs, which is regulated by both mechanical stimuli and HIF-1α activation. TGFβ1 and TGFβ2 increased LOX levels as a function of concentration and time. Inhibiting the TGFβ type I receptor (TGFβRI) decreased TGFβ2-induced LOX production by C3H10T1/2 MSCs. Low (5 mPa) and high (150 mPa) magnitudes of fluid shear stress were applied to test impacts of mechanical stimuli, but without TGFβ2, loading alone did not alter LOX levels. Low loading (5 mPa) with TGFβ2 increased LOX at 7 days greater than TGFβ2 treatment alone. Neither HIF-1α knockdown (siRNA) nor activation ($CoCl_2$) affected LOX levels. Ultimately, results suggest that TGFβ2 and appropriate loading magnitudes contribute to LOX production by C3H10T1/2 MSCs. Potential application of these findings includes treatment with TGFβ2 and appropriate mechanical stimuli to modulate LOX production by stem cells to ultimately control collagen matrix stiffening and support functional tendon formation.

Keywords: tendon, mesenchymal stem cells, lysyl oxidase, collagen crosslinking, tendon tissue engineering, mechanical loading

Introduction

Tendons transfer forces from muscle to bone and are essential to normal physiological movement. The complex hierarchical arrangement of collagen fibrils in tendon contributes to force transmission and to the unique viscoelastic properties of tendon.[1] When mechanically loaded, collagen fibrils in tendon may stretch or slide against each other to transfer mechanical forces throughout the entire tissue and distribute it among collagen fibril bundles (ie, fibers).[2–4] Sliding of the collagen fibrils and fibers may expose the tendon cells to shear stresses, resulting in increased collagen crosslinking.[5] Collagen crosslinking within and between fibrils contributes to tendon function and has recently been discussed in detail.[6,7] Briefly, collagen crosslinking impacts tendon tissue strength,[8,9] failure strain,[10] and overall fibril toughness[11] by forming bonds between collagen molecules within the fibril network.[12] Lysyl oxidase (LOX) is an enzyme, produced by cells, that is the primary mediator of enzymatic collagen crosslinking.[13,14] Both LOX levels and the products of LOX-mediated crosslinking are commonly used measures of the collagen crosslinking profile and crosslinking potential.[6,15,16]

Inhibiting LOX impairs the mechanical properties of developing tendon both in vivo and in vitro, demonstrating the critical role LOX plays in tissue formation.[16–18] Similarly,

[1]Department of Chemical & Biological Engineering, University of Idaho, Moscow, Idaho, USA.
[2]Department of Mechanical Engineering, University of Idaho, Moscow, Idaho, USA.

exogenous treatments with LOX or LOX-like 2 (LOXL2) protein enhances tissue mechanical properties.[19–21] Thus, tendon tissue engineering approaches could benefit from control of LOX levels during tissue formation to modulate collagen crosslinking and mechanical properties. One possible way to control LOX levels is through regulation of LOX production by the cells used in a tissue engineering approach. Despite the prevalence of mesenchymal stem cells (MSCs) being explored for tissue engineering strategies, the specific mechanisms governing their LOX production is poorly understood. Significant knowledge gaps remain regarding how commonly tested factors for tendon formation including mechanical loading, hypoxia, and growth factor signaling impact MSCs. Identifying the regulators of LOX production by MSCs is imperative to developing regenerative strategies targeted at controlling functional tendon formation.

Potential regulators of LOX production may be the transforming growth factor (TGF)βs,[7,22–24] which are multifunctional cytokines that impact tendon development and healing. TGFβ1 is prevalent in tendon injury, healing and fibrosis, and upregulates *LOX* levels in nontendon cells.[22,23] TGFβ2 is a potent inducer of tenogenic differentiation[25–32] and is necessary for tendon formation.[31,33] Recently, TGFβ2 upregulated tendon markers in murine tendon progenitor cells to a higher degree compared with TGFβ1.[34] TGFβ1 and TGFβ2 can potentially activate downstream TGFβ cell signaling through the TGFβ type I receptor (TGFβRI) in tendon.[35] Further, TGFβ family signaling can be mechanically activated to promote tendon-specific matrix. However, the impact of TGFβ1 and TGFβ2 on LOX production in MSCs has not been explored.

Mechanical loading has also been shown to be a potential regulator of LOX.[5,18,36,37] For example, human periodontal ligament-derived (hPDL) cells increased *LOX* gene expression under low tensile strain but not under higher magnitudes.[36] Similar observations were noted under low and high compressive loads.[37] Work in embryonic chick tendon comparing paralysis and hypermotility showed that paralysis (diminished loading) decreases both LOX activity and elastic modulus of the chick calcaneal tendon.[18] These studies emphasize that LOX may be mechanosensitive, but specific cellular mechanisms and pathways were not explored.

Hypoxia, or low oxygen conditions, may also affect LOX production. Notably, application of a hypoxic environment increased *LOX* gene expression in bovine cartilage explants,[38] but activation of hypoxia-inducible factor (HIF)-1α, a transcription factor upregulated by hypoxic conditions,[39] was not specifically explored. HIF-1α has been shown to increase during mechanical stimuli in tendon fibroblasts[40] and promote tenogenic markers (tenomodulin and decorin) and patellar tendon repair using rabbit-derived MSCs.[41] Although hypoxia and HIF-1α appear to be possible regulators of LOX and tenogenesis (differentiation toward the tendon lineage), impacts of HIF-1α activation on LOX production by MSCs remain unknown.

Therefore, the objective of this study was to elucidate the role of TGFβ signaling (TGFβ1 and TGFβ2) in LOX production and further investigate mechanical stimuli and HIF-1α as additional regulators of LOX in a well-established multipotent MSC line (C3H10T1/2). We hypothesized that TGFβ signaling promotes LOX activity, which is regulated by both mechanical stimuli and HIF-1α activation. To test this hypothesis, we treated C3H10T1/2 MSCs with TGFβ1 and TGFβ2, a small molecule inhibitor of TGFβRI, applied fluid shear stress, and used siRNA to knockdown HIF-1α to determine impacts on LOX production.

Materials and Methods

Cell culture and supplementation

The murine C3H10T1/2 (ATCC, Manassas, VA) MSC line was cultured in standard growth medium (Dulbecco's modified Eagle's medium [DMEM], 10% fetal bovine serum [FBS], and 1% penicillin/streptomycin). C3H10T1/2 MSCs were seeded into 12-well or 6-well plates at a density of 20,000 cells/cm^2 (passage 3–13) and incubated for 24 h to allow for cell attachment. C3H10T1/2 MSCs were washed with warmed phosphate buffered saline (PBS; Gibco, Grand Island, NY), switched to reduced FBS medium (DMEM, 1% FBS, 1% penicillin/streptomycin), and incubated for another 24 h before treatment. Cells were again rinsed with warm PBS and then treated with recombinant human TGFβ1 or TGFβ2 (PeproTech, Rocky Hill, NJ) (0.1–100 ng/mL) and compared against vehicle controls (VCs) of citric acid or sterile water, as recommended by the manufacturer for reconstitution of the lyophilized TGFβ1 and TGFβ2 proteins, respectively. TGFβRI-dependent signaling was interrogated with 10 μM SB431542 (R&D Systems, Minneapolis, MN), a selective chemical TGFβRI inhibitor,[42] with DMSO as the VC. Cells were cultured for 1, 3, and 7 days (d) ($n = 3$) with media changes every 3 days. Experiments using mechanical loading or interrogating HIF-1α were treated with 50 ng/mL TGFβ2 to more deeply evaluate the role of TGFβ2, which is already established as a tenogenic factor.[26–29,43] Cell morphology was qualitatively assessed using phase-contrast microscopy and DAPI/phalloidin staining (Supplementary Data S1).

Mechanical loading

Mechanical loading was applied to C3H10T1/2 MSCs in 6-well plates via fluid shear stress using an orbital shaker plate running at either low magnitude (0.1 Hz) or high magnitude (1 Hz) for 4 h/day (Lab-Line Instruments Inc., Melrose Park, IL) in the cell culture incubator (Supplementary Data S2). Fluid shear stress was applied to model the shear stresses that may be experienced by tendon cells in vivo.[5,44] Static conditions (no loading) served as controls. Fluid shear stress was estimated by modeling the system as flow near an infinite rotating disk (with laminar and homogenous flow) and applying the circumferential wall shear stress on a disk equation[45] (Equation 1):

$$\tau = \rho \cdot r \cdot G_0' \cdot \sqrt{\nu\omega^3}, \qquad \text{(Equation 1)}$$

where density (ρ) and kinematic viscosity (ν) of the culture media were simplified as the properties of water at room temperature.[46] The radius (r) was measured from the well, and angular velocity (ω) was set on the orbital shaker plate. These parameters are described in more detail in Supplementary Data S2.

Low and high magnitude loading shear stresses (τ) were calculated to be 4.8 mPa (~5 mPa) and 151 mPa (~150 mPa), respectively (Supplementary Data S2). Selected loading

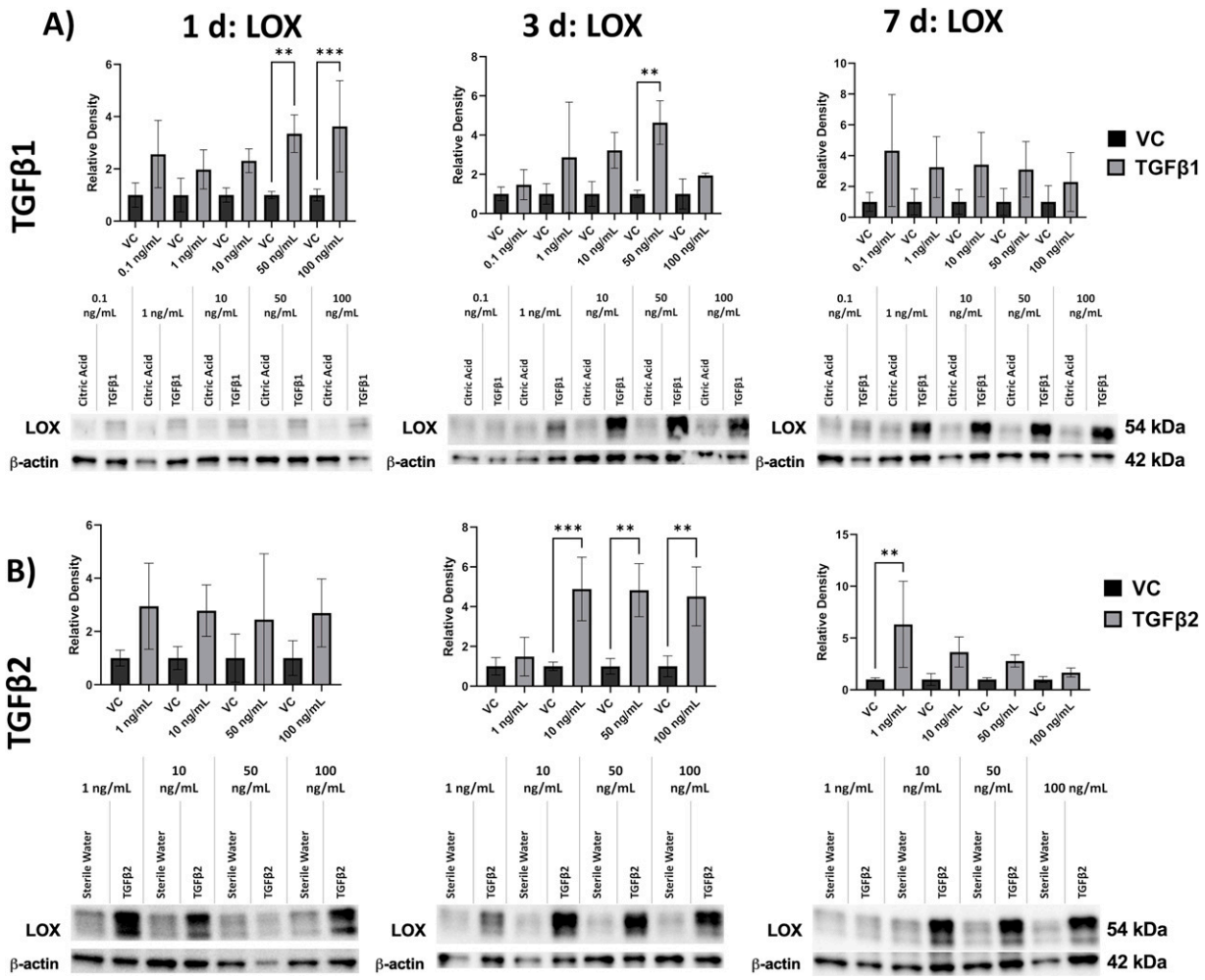

FIG. 1. Impact of transforming growth factor (TGF)β1 and TGFβ2 on lysyl oxidase (LOX) production by C3H10T1/2 mesenchymal stem cells (MSCs). Western blot densitometry for LOX after 1, 3, and 7 d of **(A)** 0.1–100 ng/mL TGFβ1 and **(B)** 1–100 ng/mL TGFβ2 treatment. TGFβ1 and TGFβ2 increase LOX levels as a function of time and concentration, compared with their vehicle controls (VC). Representative LOX (54 kDa) and β-actin (42 kDa) western blot bands are shown below each graph.

magnitudes and durations were determined through preliminary testing (Supplementary Data S3). Higher loading durations (eg, 24 h/day) and shear stress resulted in cell death by 7 d (Supplementary Data S4).

RNAi transfection

HIF-1α was selectively silenced using TriFECTa RNAi (IDT Technologies, Coralville, IA). Three siRNA constructs and concentrations were initially tested, and 10 nM was determined most effective while maintaining cell viability. C3H10T1/2 MSCs were transfected with lipofectamine RNAiMAX (Invitrogen, Carlsbad, CA) in 6-well plates at a density of 20,000 cells/cm^2, with a universal scrambled siRNA construct (Scrambled) as a control. Treated samples were compared against 0.1 mM $CoCl_2$ (a known chemical inducer of HIF-1α[47]) (Sigma-Aldrich, St. Louis, MO), Scrambled, and VCs (Supplementary Data S5). Treatment concentration of $CoCl_2$ was determined via additional experiments (Supplementary Data S6).

Western blot analysis

Cells were collected and prepared for western blotting (WB) as previously described.[26] Briefly, cells were collected using RIPA cell lysis buffer and HALT protease inhibitor (Invitrogen, Carlsbad, CA), treated with sodium dodecyl sulfate (SDS) (1:1 ratio), sonicated and heated (95°C for 5 min) before blotting. Loading volume was adjusted to account for differences in total protein from TGFβ-induced cell proliferation (1 d = 20 μL, 3 d = 15 μL, 7 d = 10 μL). Primary rabbit antibodies were purchased for LOX, HIF-1α (Cell Signaling Technologies, Danvers, MA), and β-actin (Abcam, Cambridge MA) and used at concentrations between 1:1,000 and 1:10,000. Secondary goat anti-rabbit HRP-linked antibody (Invitrogen) was used before chemiluminescence imaging (Syngene, Frederick, MD). Blots were analyzed using band densitometry in ImageJ (NIH, Bethesda, MD). Proteins (LOX, HIF-1α, β-actin) were initially normalized to the highest intensity band on their respective blot and subsequently normalized to β-actin.

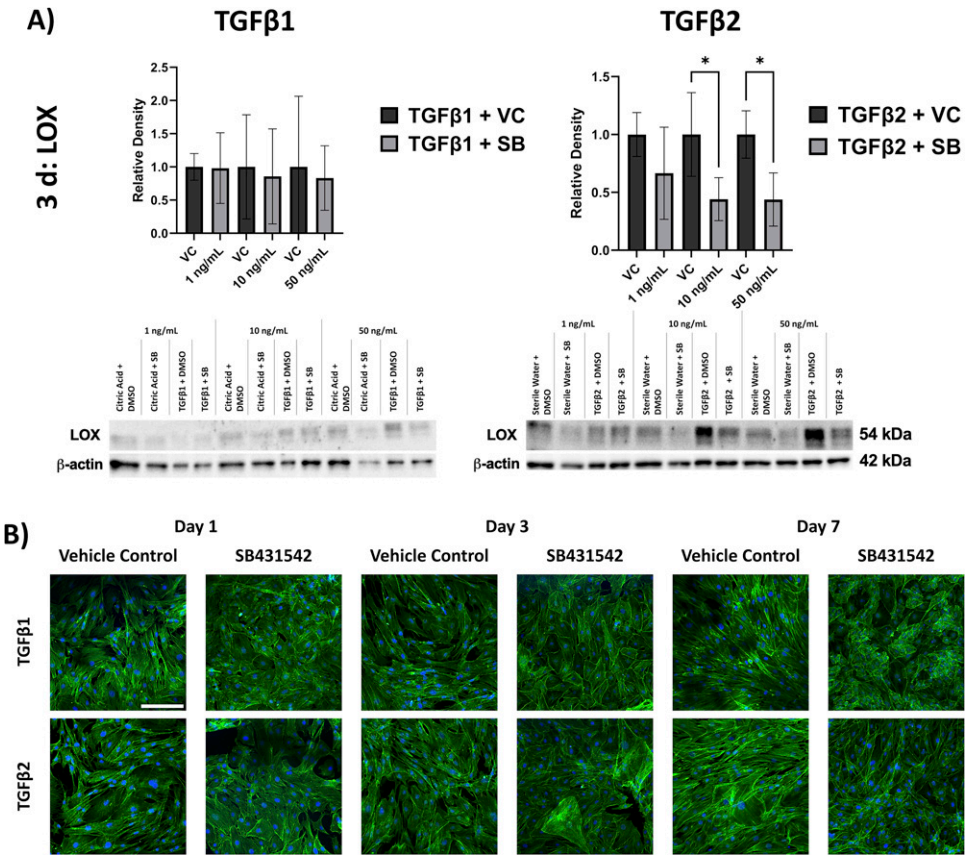

FIG. 2. Role of TGFβRI in TGFβ-induced LOX production. **(A)** Western blot densitometry for LOX after 3 d of treatment with 1, 10, or 50 ng/mL of TGFβ1 or TGFβ2, and with 10 μM of the TGFβRI inhibitor, SB431542 (SB), or DMSO, water, or citric acid as the vehicle controls (VC). TGFβRI inhibition reduced LOX levels associated with TGFβ2 treatment. Representative LOX (54 kDa) and β-actin (42 kDa) western blot bands are shown below each graph. **(B)** Fibroblastic cell morphology (*blue* = nuclei, *green* = actin cytoskeleton) associated with TGFβ1 and TGFβ2 treatment is altered with SB431542 inhibition of TGFβRI. Scale bar = 200 μm.

Statistical analysis

Technical duplicates were averaged for each experimental run ($n = 3$) and then further normalized to their same timepoint VCs or static controls (eg, 1 d static VC). TGFβ dose and TGFβRI inhibition experiments were normalized to the respective VCs and analyzed using an ordinary one-way analysis of variance (ANOVA) and Šídák's multiple-comparisons post hoc test with single pooled variance. TGFβ2 treatment with loading results were analyzed using an ordinary two-way ANOVA and Tukey's multiple-comparisons post hoc test, with a single pooled variance or multiple unpaired standard *t*-tests (Prism 9, GraphPad, La Jolla, CA). Significance was considered to be $P < 0.05$.

Results

TGFβ increased LOX production as function of isoform, concentration, and time, and inhibiting TGFβRI impaired LOX induction by TGFβ2 signaling

Treatment with TGFβ1 and TGFβ2 increased LOX production relative to controls, depending on concentration and time (Fig. 1). At 1 d, LOX levels increased with 50 ng/mL ($P < 0.002$) and 100 ng/mL ($P < 0.001$) of TGFβ1 (Fig. 1A). At 3 d, LOX levels trended upward with 10 ng/mL TGFβ1 ($P = 0.053$) and increased at 50 ng/mL ($P < 0.003$) (Fig. 1A), whereas LOX levels increased with TGFβ2 treatment at 10 ng/mL ($P < 0.001$), 50 ng/mL ($P < 0.01$), and 100 ng/mL ($P < 0.01$) (Fig. 1B). At 7 d, LOX was increased by 1 ng/mL TGFβ2 ($P = 0.01$) (Fig. 1B). Neither TGFβ1 nor TGFβ2 had a clear impact on LOX levels at early timepoints (30 min or 1 h) after treatment (Supplementary Data S7).

Inhibition of TGFβRI with SB431542 impaired LOX increases when treated with 10 ng/mL ($P < 0.05$) and 50 ng/mL ($P < 0.05$) TGFβ2 at 3 d (Fig. 2A). Interestingly, TGFβRI inhibition minimally impacted the TGFβ1-induced increases in LOX (Fig. 2A). TGFβRI inhibition impaired the fibroblastic morphological changes in C3H10T1/2 MSCs that are typically associated with TGFβ treatment and shifted the cells toward a more spread-out morphology compared with the TGFβ and DMSO VCs at all timepoints (Fig. 2B).

TGFβ2 increased LOX and HIF-1α activity, with differential regulation by low-(5 mPa) and high-(150 mPa) magnitude fluid shear stress

Based on the finding that TGFβ2 can induce LOX activity (Figs. 1 and 2), prior work demonstrating the tenogenic potential of TGFβ2[25–29,34,43,48] and our prior work showing enhanced tenogenesis of C3H10T1/2 MSCs with 50 ng/mL

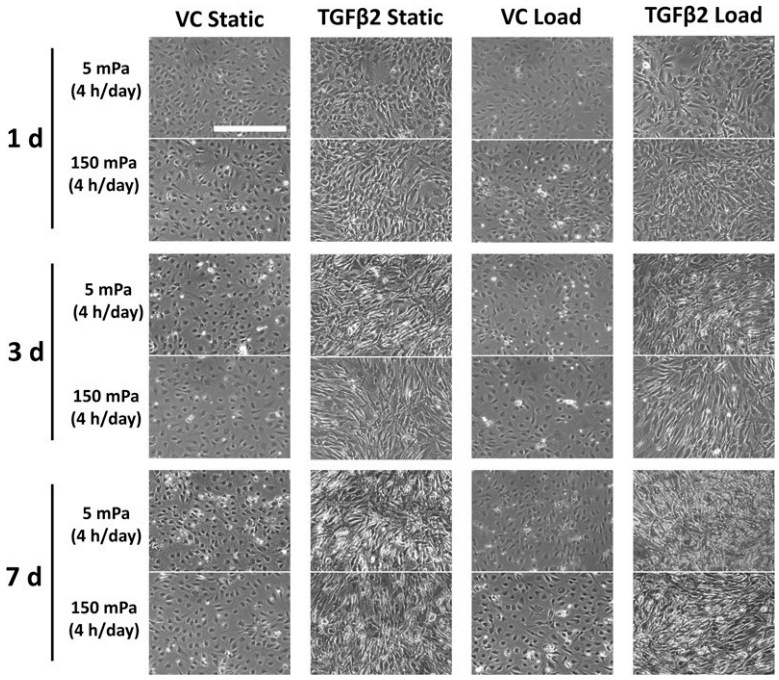

FIG. 3. Phase-contrast images of C3H10T1/2 MSCs treated with TGFβ2 and mechanical stimuli. Representative phase-contrast images (10×) showing cell morphology for TGFβ2, or vehicle control (VC) treated cells that were exposed to mechanical stimuli (Load) or static control (Static) conditions at 1 d, 3 d, and 7 d timepoints. TGFβ2-associated changes (eg, fibroblastic morphology) were observed, but no obvious changes were associated with loading. Scale bar = 400 μm.

TGFβ2,[26,27] 50 ng/mL TGFβ2 was selected for all subsequent experiments. Morphological changes typically associated with 50 ng/mL TGFβ2 treatment (eg, fibroblastic cell morphology)[26,27] were observed in C3H10T1/2 MSCs at all timepoints (Fig. 3, Supplementary Data S1). Fluid shear stress did not appear to significantly affect cell morphology compared with static controls (Fig. 3). In the 5 mPa experiments, static TGFβ2 treatment increased LOX at 1 d ($P < 0.01$), 3 d ($P < 0.0001$), and 7 d ($P < 0.01$) compared with static VCs (Fig. 4A). Static TGFβ2 treatment increased HIF-1α activity at 1 d ($P < 0.05$) (Fig. 5A), but HIF-1α was not reliably detected at 3 d or 7 d timepoints. The 150 mPa experiments confirmed these same trends, where static TGFβ2 treatment increased LOX at 1 d ($P < 0.01$), 3 d ($P < 0.05$), and 7 d ($P < 0.01$) compared with static VCs (Fig. 4B). Again, static TGFβ2 treatment increased HIF-1α activity at 1 d ($P < 0.05$) (Fig. 5B), but HIF-1α was not reliably detected at subsequent timepoints.

A statistically significant interaction between TGFβ2 treatment and loading ($P < 0.01$) was identified at 3 d, where static TGFβ2 treatment increased LOX levels over TGFβ2 with 5 mPa loading ($P < 0.05$). Interestingly, this trend was reversed at 7 d. TGFβ2 with low loading (5 mPa) increased LOX levels greater than static TGFβ2 treatment ($P < 0.01$) and greater than static ($P < 0.0001$) and loaded VCs ($P < 0.0001$) (Fig. 4A). A significant interaction was also observed between TGFβ2 treatment at 7 d ($P < 0.01$). Higher loading magnitudes (150 mPa) (Fig. 4B) and other loading durations (eg, 12 h/day) did not affect LOX production, relative to static TGFβ2 controls (Supplementary Data S3). HIF-1α was not affected by loading conditions but was detectable at 1 d with TGFβ2 treatment (Fig. 5).

siRNA HIF-1α knockdown and chemical induction ($CoCl_2$) of HIF-1α suggest that LOX activity is independent of HIF-1α

To knockdown HIF-1α, cells were transfected with siRNA or a scrambled control construct (Scrambled) and treated with either TGFβ2 or $CoCl_2$ (to chemically induce HIF-1α) and cultured for 1 d (Supplementary Data S5, S6). $CoCl_2$ effectively induced HIF-1α activity 70-fold, relative to scrambled VC ($P < 0.0001$) and siRNA groups ($P < 0.0001$) (Fig. 6A). The HIF-1α siRNA transfection was validated by successful reduction of HIF-1α activity in the presence of both $CoCl_2$ ($P < 0.0001$) and TGFβ2 ($P < 0.05$) HIF-1α activators compared with their respective controls (Fig. 6C). LOX production was not significantly affected by HIF-1α induction (with $CoCl_2$) ($P = 0.39$) or by HIF-1α knockdown ($P = 0.61$) compared with controls (Fig. 6B). Similarly, TGFβ2-induced LOX production was not affected by HIF-1α knockdown ($P = 0.90$).

Discussion

Collagen crosslinking is essential for normal tendon development and function. However, cellular regulators of the enzymes that impact collagen crosslinking remain unknown in MSCs, which is a challenge for strategies that employ stem cells for tissue engineering. Here, we demonstrated that TGFβ1 and TGFβ2 promote LOX production by C3H10T1/2 MSCs, as a function of TGFβ isoform, concentration, and time. For TGFβ2, this impact appeared to be mediated by TGFβRI. When mechanical stimuli and TGFβ2 were explored in combination, LOX levels increased with low magnitude shear stress (5 mPa) at 7 d but not higher magnitudes (150 mPa) or at other timepoints. In all cases, TGFβ2 was required, as mechanical stimuli alone did not induce LOX production. Neither HIF-1α knockdown nor activation showed an obvious role of HIF-1α activation on LOX production. Altogether, these data suggest that TGFβ2 signaling via TGFβRI and specific magnitudes and timing of mechanical stimuli regulate LOX production by C3H10T1/2 MSCs, which has implications for regulating collagen crosslinking and directing tissue engineered tendon development.

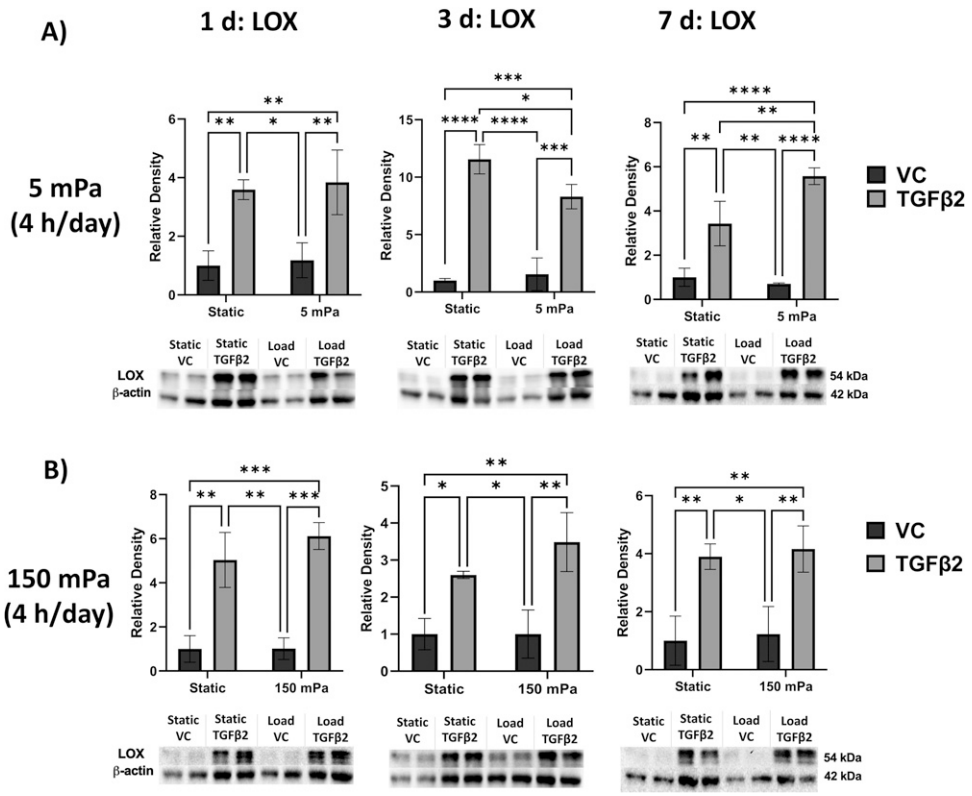

FIG. 4. LOX production by C3H10T1/2 MSCs treated with TGFβ2 and mechanical stimuli. Western blot densitometry for LOX, with representative LOX (54 kDa) and β-actin (42 kDa) western blot bands shown below each graph for **(A)** 5 mPa and **(B)** 150 mPa loading conditions. Representative blots show technical replicates. TGFβ2 increased LOX at all timepoints and loading conditions. Notably, TGFβ2 combined with 5 mPa at 4 h/day increased LOX greater than TGFβ2 treatment alone at 7 d, demonstrating a statistically significant interaction between TGFβ2 and loading.

The TGFβ family plays an important role in connective tissue development and function. Knocking out TGFβ2 and TGFβ3 impairs tendon formation during mouse embryonic development,[33] and TGFβ1 knockout mice have impaired late-stage wound healing.[49] TGFβ2 is a potent inducer of tenogenesis in embryonic tendon cells[28,29] and MSCs[26,27] and is present in tendon throughout embryonic chick development.[43] In different cell types, TGFβ1 is a well-known inducer of enzymatic crosslinks in fibrotic conditions and scar formation.[24,50] However, the exact relationship between TGFβ signaling and collagen crosslinking enzyme activity in C3H10T1/2 MSCs remained obscured until this point.

To the best of our knowledge, this is the first study in C3H10T1/2 MSCs, which further implicates TGFβ2 as a potent stimulator of LOX production via TGFβRI. Our findings corroborate similar work in human trabecular meshwork cells connecting the TGFβ family with increased *LOX* and *LOX-like proteins* (*LOXL1-4*) via TGFβRI and-II signaling through canonical Smad and noncanonical (MAPK/JNK, AP-1) pathways.[22] Together, this work describes TGFβ2 as a key regulator of LOX, which is critical to collagen crosslinking and tendon development.[15,16] Future studies will explore both canonical and noncanonical pathways as potential signaling mechanisms for TGFβ2-induced LOX production in tendon cells and MSCs.

Mechanical loading of tendon exerts a shear stress on tendon cells due to fluid transfer and sliding between collagen fibrils and fibers. Although exact shear stresses are unknown in vivo, estimates range from 0.1 to 65 mPa via fluid flow.[5,51,52] Further, fluid shear stresses of 14–60 mPa maintain scleraxis expression in tendon cells in vitro.[44] We applied fluid shear stress at low (5 mPa) and high (150 mPa) loading magnitudes for 4 h/day. Low loading magnitudes increased LOX levels but only when combined with TGFβ2 treatment at 7 d, whereas other magnitudes (150 mPa) and timepoints did not. We suspect that 7 d of TGFβ2 treatment increased tenogenesis (characterized by increased fibroblastic cell morphology [Figs. 2-3, Supplementary Data S1] and prior work showing increased tendon markers with TGFβ2 treatment[26,27]) and may have altered cell mechanosensitivity. Similar work in hPDL cells has shown that *LOX* and collagen expression respond in magnitude-dependent manners to mechanical loading, with lower magnitudes increasing *LOX* and collagen compared with higher magnitudes of loading.[36,37] Taken together, lower magnitudes of mechanical stimulation may promote stabilization of the extracellular matrix (ECM) through enhanced LOX-mediated crosslinking, whereas higher magnitudes may favor ECM remodeling. A similarly adaptive phenomenon may explain why low shear stress (5 mPa) initially reduced LOX at 3 d before increasing LOX activity at 7 d to first remodel and then stabilize the collagen matrix. Ultimately, this work describes a mechanical loading-based mechanism to modulate LOX production in C3H10T1/2 MSCs, which could be used in future tissue engineering approaches.

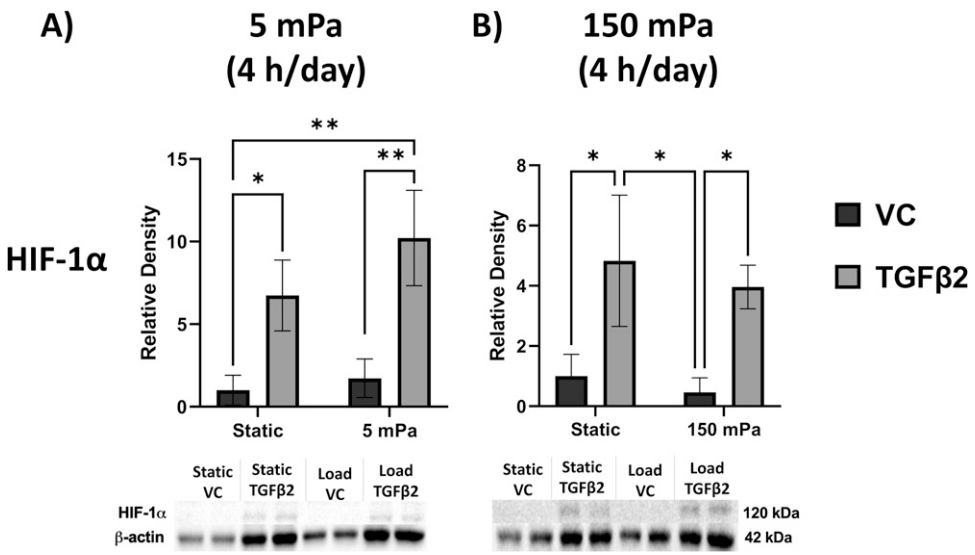

FIG. 5. Hypoxia-inducible factor (HIF)-1α levels in C3H10T1/2 MSCs treated with TGFβ2 and mechanical stimuli at 1 d. Western blot densitometry for HIF-1α at 1 d, with representative HIF-1α (120 kDa) and β-actin (42 kDa) western blot bands shown below each graph for **(A)** 5 mPa and **(B)** 150 mPa loading conditions. Representative blots show technical replicates. TGFβ2 increased HIF-1α activity at 1 d and under all loading conditions, but no effects of loading on HIF-1α were observed. HIF-1α was not reliably detected after 1 d.

Although HIF-1α activation has been proposed as a regulator of LOX production in other musculoskeletal tissues,[38] our results do not persuasively identify it as a primary regulator of TGFβ2-induced LOX activity in C3H10T1/2 MSCs. Hypoxia, a known HIF-1α activator, was previously shown to increase *LOX* gene expression, mechanical strength, and pyridinoline crosslinks in bovine articular cartilage explants.[38] In the context of our findings, it appears that hypoxia may modulate LOX and tissue development through mechanisms other than HIF-1α activation, which is

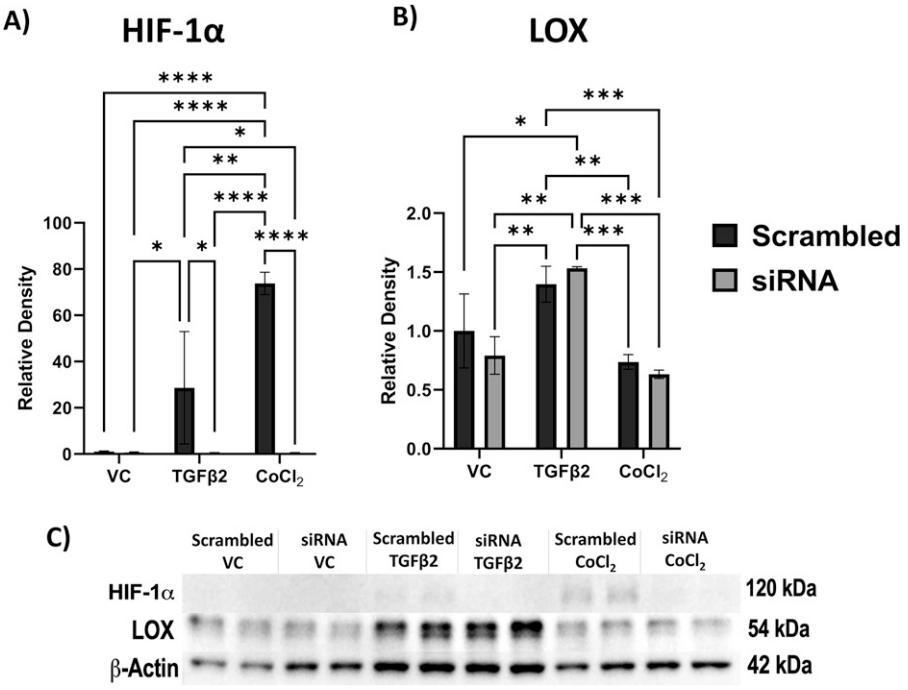

FIG. 6. LOX production in C3H10T1/2 MSCs with siRNA knockdown of HIF-1α and $CoCl_2$ activation of HIF-1α. Western blot densitometry for LOX or HIF-1α at 1 d, following either siRNA treatment to knockdown HIF-1α or $CoCl_2$ activation of HIF-1α. **(A)** $CoCl_2$ effectively induced HIF-1α activity, resulting in a 70-fold increase relative to scrambled vehicle control (VC) and siRNA (siRNA) groups. siRNA treatment effectively reduced HIF-1α levels compared with VC and positive ($CoCl_2$) controls. **(B)** LOX levels were not affected by HIF-1α activation or knockdown. **(C)** Representative HIF-1α (120 kDa, LOX (54 kDa, and β-actin (42 kDa) western blot bands showing technical replicates.

supported by LOX activity being independent of HIF-1α activation ($CoCl_2$) or knockdown (siRNA). Inducing a hypoxic environment with low oxygen, rather than chemically via HIF-1α activation by $CoCl_2$, may provide more insight into the potential role of hypoxia on crosslinking or LOX activity in tenogenic MSCs. It is possible that there is a discrepancy between the regulation of *LOX* gene expression and LOX activity that could be due to the complex maturation processes that yield catalytically active LOX.

This study is limited by the collection of relatively early timepoints (≤7 d of treatment) when the C3H10T1/2 MSCs are not yet fully differentiated, whereas later stages of tenogenic differentiation may yield different results. Further, this work was conducted in a model murine MSC line (C3H10T1/2), which may be predisposed toward a fibroblastic morphology and may limit applications to other lineages. Although C3H10T1/2 MSCs are commonly used to study differentiation[53,54] and tenogenesis[26,27,55–57] and here provide an initial understanding of LOX regulators, future work will also need to investigate these mechanisms in more clinically relevant adult human MSCs as well as primary tendon cells and tendon progenitors. However, a prior study showed that tendon progenitor cells and adult MSCs had similar tenogenic responses to TGFβ2, suggesting shared mechanisms,[28] but this will be explored in future investigations of LOX production. A recent study showed that exogenous LOX treatments had minimal impact on embryonic tendon cells,[58] but additional studies are needed to explore how LOX production changes throughout tenogenesis or impacts differentiation. In addition, our selected mode of mechanical stimuli and maximum applied shear stress (150 mPa) may limit the scope of this study as it was greater than some in vivo estimates[44] but still below others (5 Pa).[5] It is also unknown if the magnitude of shear stress changes throughout tissue formation or impacts differentiation. This initial study used 2D culture, and future studies will use a 3D environment to provide additional developmental cues (eg, cell-binding motifs) and to measure the formation of LOX-mediated collagen crosslinks. Finally, as cells in tendon also experience tensile and compressive loading, these modes of mechanical stimuli will be applied to stem cells in future 3D models to better understand the mechanical regulators of collagen crosslinking formation.

Conclusions

Ultimately, we have demonstrated that TGFβs enhance LOX production in C3H10T1/2 MSCs. TGFβ2 appears to be a potent regulator of LOX levels and acts through TGFβRI. LOX production appears to be independent of mechanical stimuli when applied in isolation and requires TGFβ2, and lower levels of shear stress with TGFβ2 treatment promoted LOX production at 7 d. Further, LOX production was not altered by changes in HIF-1α activation, which contrasts previous work showing that hypoxia promotes *LOX* gene expression. Together, these findings contribute to a growing body of evidence defining the critical role of TGFβ2 in LOX production. Long-term implications may include the application of TGFβ2 and appropriate magnitudes of mechanical loading at targeted timepoints to control collagen crosslinking formation to guide tissue development.

Author Disclosure Statement

The authors declare no conflict of interest.

Funding Information

This project was made possible by an Idaho NASA EPSCoR Research Initiation Grant, National Science Foundation Grant No. 2145004, INBRE program, P20GM103408 (National Institutes of General Medical Sciences), and Beckman Scholars Award from the Arnold and Mabel Beckman Foundation (to N.M.P.).

Supplementary Material

Supplementary Data S1
Supplementary Data S2
Supplementary Data S3
Supplementary Data S4
Supplementary Data S5
Supplementary Data S6
Supplementary Data S7

References

1. Provenzano PP, Vanderby R. Collagen fibril morphology and organization: Implications for force transmission in ligament and tendon. Matrix Biol 2006;25:71–84; doi: 10.1016/j.matbio.2005.09.005
2. Fang F, Lake SP. Multiscale strain analysis of tendon subjected to shear and compression demonstrates strain attenuation, fiber sliding, and reorganization. J Orthop Res 2015; 33:1704–1712; doi: 10.1002/jor.22955
3. Screen HRC, Lee DA, Bader DL, et al. An investigation into the effects of the hierarchical structure of tendon fascicles on micromechanical properties. Proc Inst Mech Eng H 2004;218:109–119; doi: 10.1243/095441104322984004
4. Szczesny SE, Elliott DM. Interfibrillar shear stress is the loading mechanism of collagen fibrils in tendon. Acta Biomater 2014;10:2582–2590; doi: 10.1016/j.actbio.2014.01.032
5. Passini FS, Jaeger PK, Saab AS, et al. Shear-stress sensing by PIEZO1 regulates tendon stiffness in rodents and influences jumping performance in humans. Nat Biomed Eng 2021;5:1457–1471; doi: 10.1038/s41551-021-00716-x
6. Eekhoff JD, Fang F, Lake SP. Multiscale mechanical effects of native collagen cross-linking in tendon. Connect Tissue Res 2018;59:410–422; doi: 10.1080/03008207.2018.1449837
7. Ellingson AJ, Pancheri NM, Schiele NR. Regulators of collagen crosslinking in developing and adult tendons. Eur Cell Mater 2022;43:130–152; doi: 10.22203/eCM.v043a11
8. Tang Y, Ballarini R, Buehler MJ, et al. Deformation micromechanisms of collagen fibrils under uniaxial tension. J R Soc Interface 2010;7:839–850; doi: 10.1098/rsif.2009.0390
9. Uzel SGM, Buehler MJ. Molecular structure, mechanical behavior and failure mechanism of the C-terminal cross-link domain in type I collagen. J Mech Behav Biomed Mater 2011;4:153–161; doi: 10.1016/j.jmbbm.2010.07.003
10. Depalle B, Qin Z, Shefelbine SJ, et al. Influence of cross-link structure, density and mechanical properties in the mesoscale deformation mechanisms of collagen fibrils. J Mech Behav Biomed Mater 2015;52:1–13; doi: 10.1016/j.jmbbm.2014.07.008

11. Buehler MJ. Nanomechanics of collagen fibrils under varying cross-link densities: Atomistic and continuum studies. J Mech Behav Biomed Mater 2008;1:59–67; doi: 10.1016/j.jmbbm.2007.04.001
12. Eyre DR, Koob TJ, Van Ness KP. Quantitation of hydroxypyridinium crosslinks in collagen by high-performance liquid chromatography. Anal Biochem 1984;137:380–388.
13. Lucero HA, Kagan HM. Lysyl oxidase: An oxidative enzyme and effector of cell function. Cell Mol Life Sci 2006;63:2304–2316; doi: 10.1007/s00018-006-6149-9
14. Pinnell SR, Martin GR. The cross-linking of collagen and elastin: Enzymatic conversion of lysine in peptide linkage to alpha-aminoadipic-delta-semialdehyde (allysine) by an extract from bone. Proc Natl Acad Sci U S A 1968;61:708–716; doi: 10.1073/pnas.61.2.708
15. Marturano JE, Arena JD, Schiller ZA, et al. Characterization of mechanical and biochemical properties of developing embryonic tendon. Proc Natl Acad Sci U S A 2013;110:6370–6375; doi: 10.1073/pnas.1300135110
16. Marturano JE, Xylas JF, Sridharan GV, et al. Lysyl oxidase-mediated collagen crosslinks may be assessed as markers of functional properties of tendon tissue formation. Acta Biomater 2014;10:1370–1379; doi: 10.1016/j.actbio.2013.11.024
17. Herchenhan A, Uhlenbrock F, Eliasson P, et al. Lysyl oxidase activity is required for ordered collagen fibrillogenesis by tendon cells. J Biol Chem 2015;290:16440–16450; doi: 10.1074/jbc.M115.641670
18. Pan XS, Li J, Brown EB, et al. Embryo movements regulate tendon mechanical property development. Philos Trans R Soc Lond B Biol Sci 2018;373:20170325; doi: 10.1098/rstb.2017.0325
19. Bates ME, Troop L, Brown ME, et al. Temporal application of lysyl oxidase during hierarchical collagen fiber formation differentially effects tissue mechanics. Acta Biomater 2023;160:98–111; doi: 10.1016/j.actbio.2023.02.024
20. Brown WE, Huang BJ, Hu JC, et al. Engineering large, anatomically shaped osteochondral constructs with robust interfacial shear properties. NPJ Regen Med 2021;6:42; doi: 10.1038/s41536-021-00152-0
21. Nguyen PK, Jana A, Huang C, et al. Tendon mechanical properties are enhanced via recombinant lysyl oxidase treatment. Front Bioeng Biotechnol 2022;10:945639; doi: 10.3389/fbioe.2022.945639
22. Sethi A, Mao W, Wordinger RJ, et al. Transforming growth factor-beta induces extracellular matrix protein cross-linking lysyl oxidase (LOX) genes in human trabecular meshwork cells. Invest Ophthalmol Vis Sci 2011;52:5240–5250; doi: 10.1167/iovs.11-7287
23. Sethi A, Wordinger RJ, Clark AF. Gremlin utilizes canonical and non-canonical TGFβ signaling to induce lysyl oxidase (LOX) genes in human trabecular meshwork cells. Exp Eye Res 2013;113:117–127; doi: 10.1016/j.exer.2013.05.011
24. Van Bergen T, Marshall D, Van de Veire S, et al. The role of LOX and LOXL2 in scar formation after glaucoma surgery. Invest Ophthalmol Vis Sci 2013;54:5788–5796; doi: 10.1167/iovs.13-11696
25. Chien C, Pryce B, Tufa SF, et al. Optimizing a 3D model system for molecular manipulation of tenogenesis. Connect Tissue Res 2018;59:295–308; doi: 10.1080/03008207.2017.1383403
26. Theodossiou SK, Tokle J, Schiele NR. TGFβ2-induced tenogenesis impacts cadherin and connexin cell-cell junction proteins in mesenchymal stem cells. Biochem Biophys Res Commun 2019;508:889–893; doi: 10.1016/j.bbrc.2018.12.023
27. Theodossiou SK, Murray JB, Hold LA, et al. Akt signaling is activated by TGFβ2 and impacts tenogenic induction of mesenchymal stem cells. Stem Cell Res Ther 2021;12:88; doi: 10.1186/s13287-021-02167-2
28. Brown JP, Galassi TV, Stoppato M, et al. Comparative analysis of mesenchymal stem cell and embryonic tendon progenitor cell response to embryonic tendon biochemical and mechanical factors. Stem Cell Res Ther 2015;6:89; doi: 10.1186/s13287-015-0043-z
29. Brown JP, Finley VG, Kuo CK. Embryonic mechanical and soluble cues regulate tendon progenitor cell gene expression as a function of developmental stage and anatomical origin. J Biomech 2014;47:214–222; doi: 10.1016/j.jbiomech.2013.09.018
30. Havis E, Bonnin MA, Esteves de Lima J, et al. TGFbeta and FGF promote tendon progenitor fate and act downstream of muscle contraction to regulate tendon differentiation during chick limb development. Development 2016;143:3839–3851; doi: 10.1242/dev.136242
31. Tan G-K, Pryce BA, Stabio A, et al. Tgfβ signaling is critical for maintenance of the tendon cell fate. eLife 2020;9:e52695; doi: 10.7554/eLife.52695
32. Koch DW, Schnabel LV, Ellis IM, et al. TGF-β2 enhances expression of equine bone marrow-derived mesenchymal stem cell paracrine factors with known associations to tendon healing. Stem Cell Res Ther 2022;13:477; doi: 10.1186/s13287-022-03172-9
33. Pryce BA, Watson SS, Murchison ND, et al. Recruitment and maintenance of tendon progenitors by TGFβ signaling are essential for tendon formation. Development 2009;136:1351–1361; doi: 10.1242/dev.027342
34. Kent RN, Jewett ME, Buck TP, et al. Engineered microenvironmental cues from fiber-reinforced hydrogel composites drive tenogenesis and aligned collagen deposition. Adv Healthc Mater 2024:e2400529; doi: 10.1002/adhm.202400529
35. Gumucio JP, Sugg KB, Mendias CL. TGF-β superfamily signaling in muscle and tendon adaptation to resistance exercise. Exerc Sport Sci Rev 2015;43:93–99; doi: 10.1249/JES.0000000000000041
36. Chen Y-J, Jeng J-H, Chang H-H, et al. Differential regulation of collagen, lysyl oxidase and MMP-2 in human periodontal ligament cells by low- and high-level mechanical stretching. J Periodontal Res 2013;48:466–474; doi: 10.1111/jre.12028
37. Kaku M, Rosales Rocabado JM, Kitami M, et al. Mechanical loading stimulates expression of collagen cross-linking associated enzymes in periodontal ligament. J Cell Physiol 2016;231:926–933; doi: 10.1002/jcp.25184
38. Makris EA, Responte DJ, Paschos NK, et al. Developing functional musculoskeletal tissues through hypoxia and lysyl oxidase-induced collagen cross-linking. Proc Natl Acad Sci U S A 2014;111:E4832–41; doi: 10.1073/pnas.1414271111
39. Wang GL, Jiang BH, Rue EA, et al. Hypoxia-inducible factor 1 is a basic-helix-loop-helix-PAS heterodimer regulated by cellular O2 tension. Proc Natl Acad Sci U S A 1995;92:5510–5514; doi: 10.1073/pnas.92.12.5510
40. Petersen W, Varoga D, Zantop T, et al. Cyclic strain influences the expression of the vascular endothelial growth factor (VEGF) and the hypoxia inducible factor 1 alpha (HIF-

1α) in tendon fibroblasts. J Orthop Res 2004;22:847–853; doi: 10.1016/j.orthres.2003.11.009
41. Chen G, Zhang W, Zhang K, et al. Hypoxia-Induced mesenchymal stem cells exhibit stronger tenogenic differentiation capacities and promote patellar tendon repair in rabbits. Sorrenti v. ed. Stem Cells Int 2020;2020:8822609–8822616; doi: 10.1155/2020/8822609
42. Inman GJ, Nicolás FJ, Callahan JF, et al. SB-431542 is a potent and specific inhibitor of transforming growth factor-beta superfamily type I activin receptor-like kinase (ALK) receptors ALK4, ALK5, and ALK7. Mol Pharmacol 2002; 62:65–74; doi: 10.1124/mol.62.1.65
43. Kuo CK, Petersen BC, Tuan RS. Spatiotemporal protein distribution of TGF-βs, their receptors, and extracellular matrix molecules during embryonic tendon development. Dev Dyn 2008;237:1477–1489; doi: 10.1002/dvdy.21547
44. Maeda T, Sakabe T, Sunaga A, et al. Conversion of mechanical force into TGF-beta-mediated biochemical signals. Curr Biol 2011;21:933–941; doi: 10.1016/j.cub.2011.04.007
45. White F. Viscous Fluid Flow. McGraw Hill; 2005. pp. 164–169.
46. Janakiraman V, Sastry S, Kadambi JR, et al. Experimental investigation and computational modeling of hydrodynamics in bifurcating microchannels. Biomed Microdevices 2008;10:355–365; doi: 10.1007/s10544-007-9143-6
47. Gao S, Zhou J, Zhao Y, et al. Hypoxia-Response Element (HRE)-directed transcriptional regulation of the rat lysyl oxidase gene in response to cobalt and cadmium. Toxicol Sci 2013;132:379–389; doi: 10.1093/toxsci/kfs327
48. Havis E, Bonnin MA, Olivera-Martinez I, et al. Transcriptomic analysis of mouse limb tendon cells during development. Development 2014;141:3683–3696; doi: 10.1242/dev.108654
49. Crowe MJ, Doetschman T, Greenhalgh DG. Delayed wound healing in immunodeficient TGF-beta 1 knockout mice. J Invest Dermatol 2000;115:3–11; doi: 10.1046/j.1523-1747.2000.00010.x
50. Fushida-Takemura H, Fukuda M, Maekawa N, et al. Detection of lysyl oxidase gene expression in rat skin during wound healing. Arch Dermatol Res 1996;288:7–10; doi: 10.1007/BF02505035
51. Ateshian GA, Costa KD, Hung CT. A theoretical analysis of water transport through chondrocytes. Biomech Model Mechanobiol 2007;6:91–101; doi: 10.1007/s10237-006-0039-9
52. Lavagnino M, Arnoczky SP, Kepich E, et al. A finite element model predicts the mechanotransduction response of tendon cells to cyclic tensile loading. Biomech Model Mechanobiol 2008;7:405–416; doi: 10.1007/s10237-007-0104-z
53. Tang Q-Q, Otto TC, Lane MD. Commitment of C3H10T1/2 pluripotent stem cells to the adipocyte lineage. Proc Natl Acad Sci U S A 2004;101:9607–9611; doi: 10.1073/pnas.0403100101
54. Ker DFE, Sharma R, Wang ETH, et al. Development of mRuby2-transfected C3H10T1/2 fibroblasts for musculoskeletal tissue engineering. Camussi G., ed. PLoS One 2015;10: e0139054; doi: 10.1371/journal.pone.0139054
55. Kataoka K, Kurimoto R, Tsutsumi H, et al. In vitro neogenesis of tendon/ligament-like tissue by combination of mohawk and a three-dimensional cyclic mechanical stretch culture system. Front Cell Dev Biol 2020;8:307; doi: 10.3389/fcell.2020.00307
56. Gaut L, Bonnin M-A, Blavet C, et al. Mechanical and molecular parameters that influence the tendon differentiation potential of C3H10T1/2 cells in 2D- and 3D-culture systems. Biol Open 2020;9:bio.047928; doi: 10.1242/bio.047928
57. Cardwell RD, Dahlgren LA, Goldstein AS. Electrospun fibre diameter, not alignment, affects mesenchymal stem cell differentiation into the tendon/ligament lineage: Ligament differentiation of C3H10T1/2 cells is enhanced on larger fibres. J Tissue Eng Regen Med 2014;8:937–945; doi: 10.1002/term.1589
58. Nguyen PK, Hall K, Holt I, et al. Recombinant lysyl oxidase effects on embryonic tendon cell phenotype and behavior. J Orthop Res 2023;41:2175–2185; doi: 10.1002/jor.25655

Address correspondence to:
Dr. Nathan R. Schiele
Department of Chemical & Biological Engineering
University of Idaho
875 Perimeter Dr. MS 0904
Moscow
ID 83843
USA

E-mail: nrschiele@uidaho.edu

Received for publication December 22, 2023
Accepted after revision May 17, 2024
Prepublished on Liebert Instant Online May 21, 2024

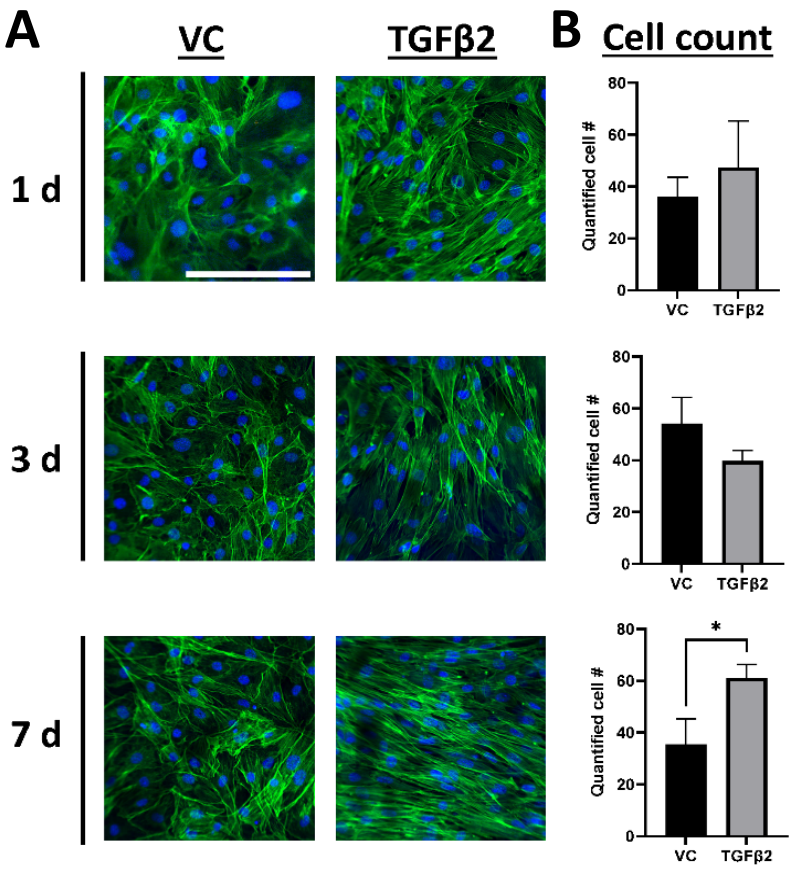

Supplemental 1. Representative 20x fluorescence images of C3H10T1/2 MSCs showing enhanced fibroblastic cell morphology with TGFβ2 treatment. **A)** Cell nuclei were stained with DAPI (blue) (Life Tech., Waltham, MA) and the actin cytoskeleton was stained with FITC-phalloidin (green) (Life Tech., Waltham, MA) and then imaged at 20x with using a spinning disk confocal microscope (Nikon, Melville, NY). Staining was conducted following fixation (10% formalin), washing (PBS), and permeabilization (0.1% Triton-X, Acros Organics). Elongated cell morphology became evident at 1 d and increased over time, resulting in fibroblastic cell morphology by 7 d. **B)** TGFβ2 significantly increased cell proliferation at 7 d, as determined by increased cell nuclei density in each image (quantified in ImageJ, NIH Bethesda, MD), compared to vehicle controls (VC) (n=3 representative images/time point). Statistical significance was determined using unpaired, two-tailed Students t-tests and $p < 0.05$ (GraphPad Prism, Boston, MA). Scale bar = 200 µm.

Supplemental 2. Fluid shear stress calculations and schematic of orbital shaker to apply fluid shear stress in culture. Calculations/tabulated data used to estimate fluid shear stress on the bottom of a cell culture well, based on the testing schematic of the applied orbital shaker plate.

<u>Supplamental 2A</u>: Orbital shaker plate test schematic

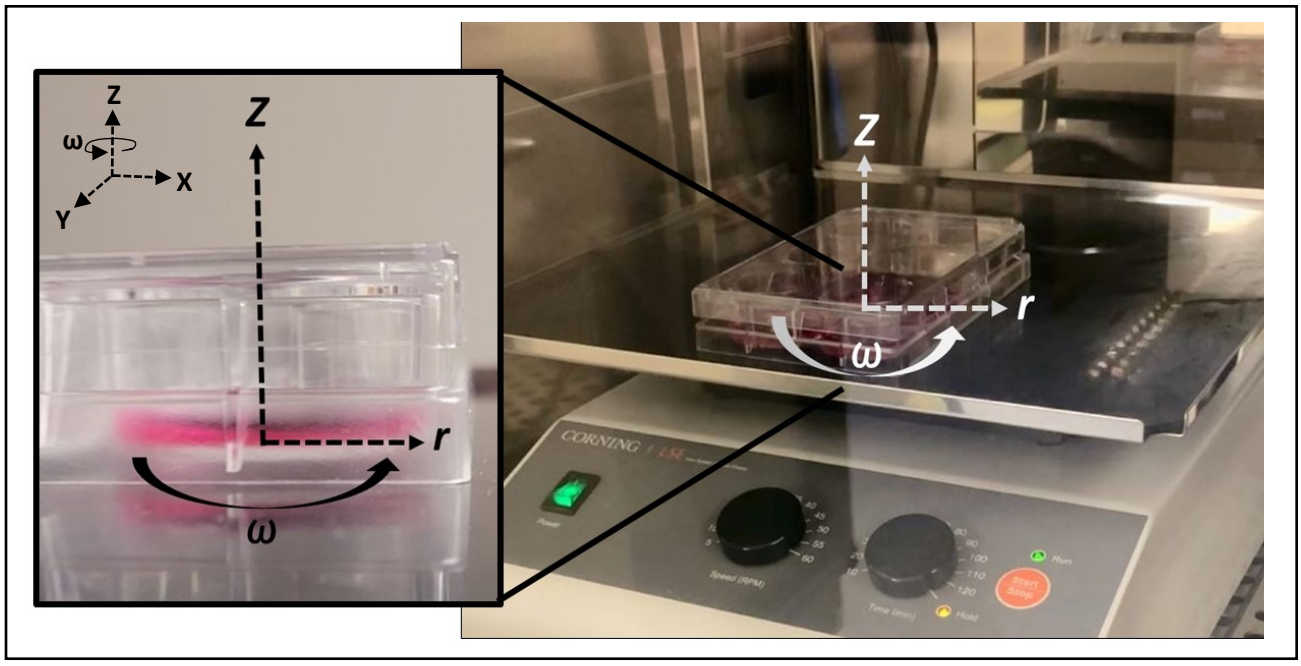

<u>Table 2</u>: Fluid fluid shear stress on the bottom of a well culture plate

RPM	**0**	**6**	**30**	**60**	**120**
f (Hz)	0.000	0.100	0.500	1.000	2.000
ω (rad/sec)	0.000	0.628	3.142	6.283	12.566
τ (Pa)	0.000	0.005	0.053	0.151	0.427
τ (mPa)	0.000	**4.777**	53.409	**151.064**	427.272
τ (dyne/cm^2)	0.000	0.048	0.534	1.511	4.273

Table 2: Parameter values used to calculate fluid shear stress

r_{6well} (m)	0.0174
ρ_{media} (kg/m^3)	1000
ν (m^2/s)	0.000000801
G'$_0$ (dimensionless)	- 0.61592
f (1/s)	set parameter
Re	238-2375

Equation 1: Circumferential wall fluid shear stress of an infinite rotating disk

$$\tau = \rho * r * G'_0 * \sqrt{\nu * \omega^3}$$

Equation 2: Circumferential wall fluid shear stress of an infinite rotating disk

$$Re = \frac{\omega * r^2}{\nu}$$

Defining Parameters:

τ is the fluid shear stress exerted on the bottom of the well plate **(Equation 1)**

ρ is the density of water at room temperature

r is the provided radius of an individual well in a 6 well culture plate

G'$_0$ is the numerical constant from tabulated data of the numerical solutions for the rotating disk[1]

ν is the kinematic viscosity of water at room temperature

ω is the angular velocity of the fluid

RPM is the set value of the orbital shaker plate and **f** is the equivalent frequency

Re is the range of Reynold's Number of the rotational flow for the tested angular velocities (**Equation 2)**

Additional Context:

Fluid shear stress on the bottom of the well was modeled as flow near an infinite rotating disk (assuming a no-slip boundary condition at the walls) per McGraw Hill Viscous Fluid Flow (Chapter: The Flow Near an Infinite Rotating Disk)[1]. Flow was considered laminar and calculated to reach a maximum ***Re*** of 2375 (at 1 Hz), well within the bounds of unstable (90,000) and turbulent (300,000) flow of an infinite rotating disc[1]. Velocity in the z-direction (the vector orthogonal to the bottom of the well) was negligible ($z^* \sim 0$), and informed selection of the dimensionless numerical constant $\mathbf{G'_0}$ (-0.61592). Physical properties (i.e., density, **ρ**, and kinematic viscosity, **ν**) of the working fluid were modeled as the primary constituent of culture media, that is, pure water. Each well was modeled with its own axis of rotational flow in the center of the well (i.e., flow rotating around the center z-axis), based upon the circular orbit of the applied shaker plate (compared to an elliptical orbit some shaker plates use).

Citations:

1. White, Frank. Viscous Fluid Flow. In: Viscous Fluid Flow. McGraw Hill, 2005, pp. 164–169.

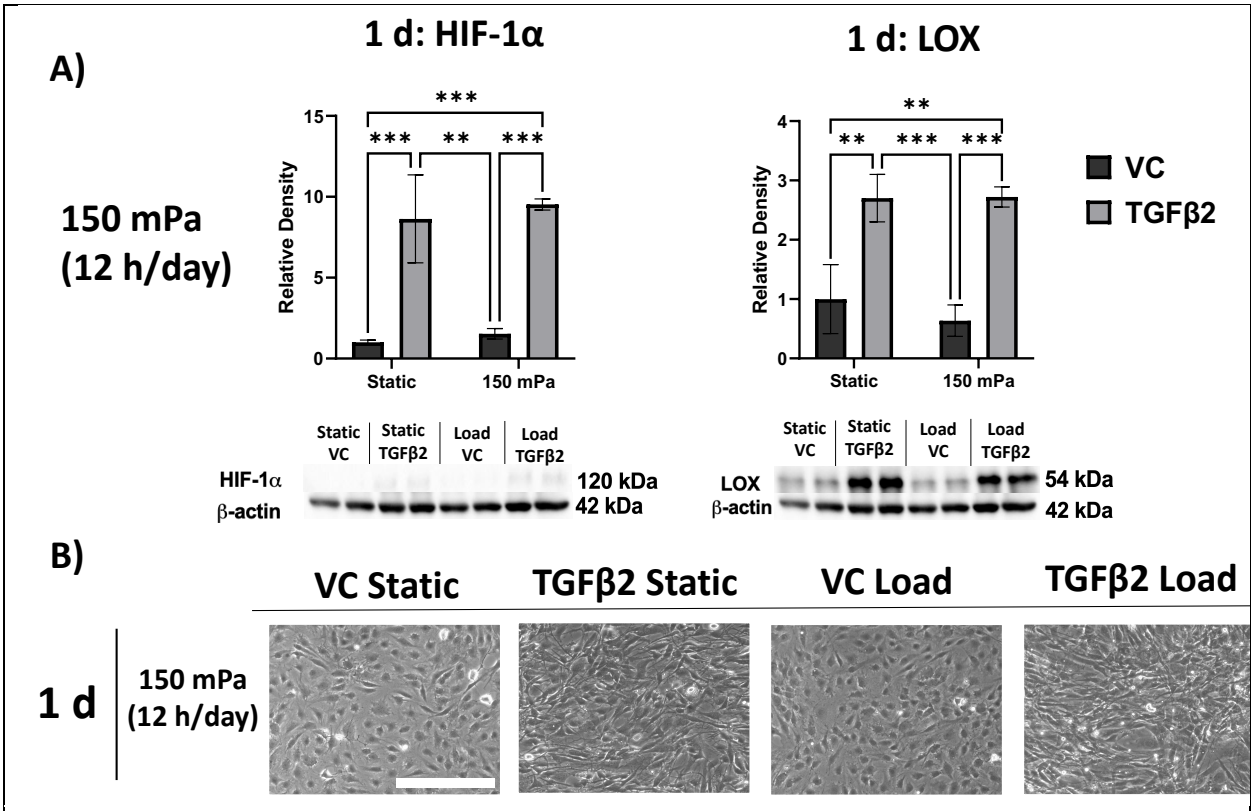

Supplemental 3. Fluid shear stress of 150 mPa applied for 12 h/day did not impact HIF-1α or LOX levels. **A)** C3H10T1/2 cells were cultured for 1 d and blotted for LOX and HIF-1α (n=3). These results (150 mPa applied for 12 h/day) corroborated the 150 mPa 4h/day at 1 d findings. Therefore, 150 mPa 4h/day loading conditions were used in the study, and later timepoints were not assessed with 12 h/day loading. Representative cell images are shown in **B).** Scale bar = 400 µm.

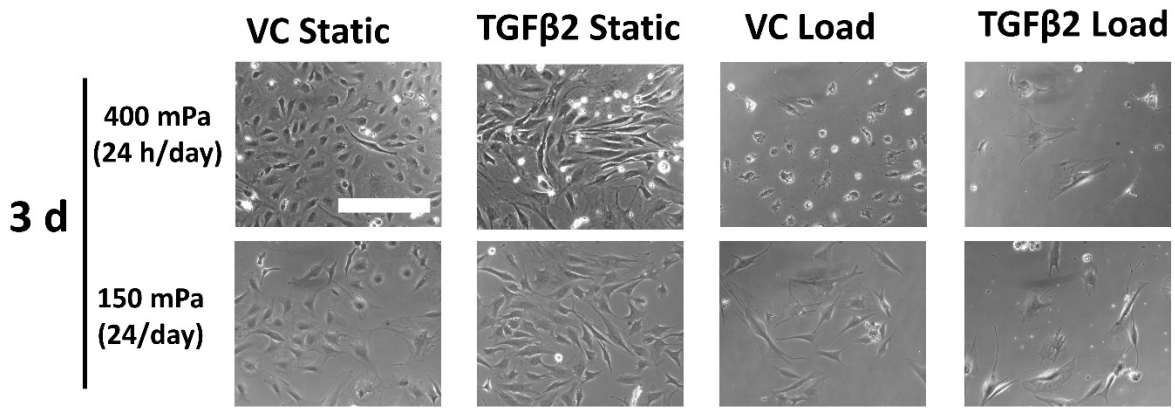

Supplemental 4. C3H10T1/2 cell viability with additional loading conditions. Additional experiments considered upper-limit loading conditions and assessed cell viability. An orbital shaker plate frequency of 2 Hz produced an estimated shear stress of 400 mPa and resulted in cell death by 3 d. Similarly, 150 mPa loading for 24 h/day appeared cytotoxic with few viable cells remaining by 3 d. Scale bar = 400 μm.

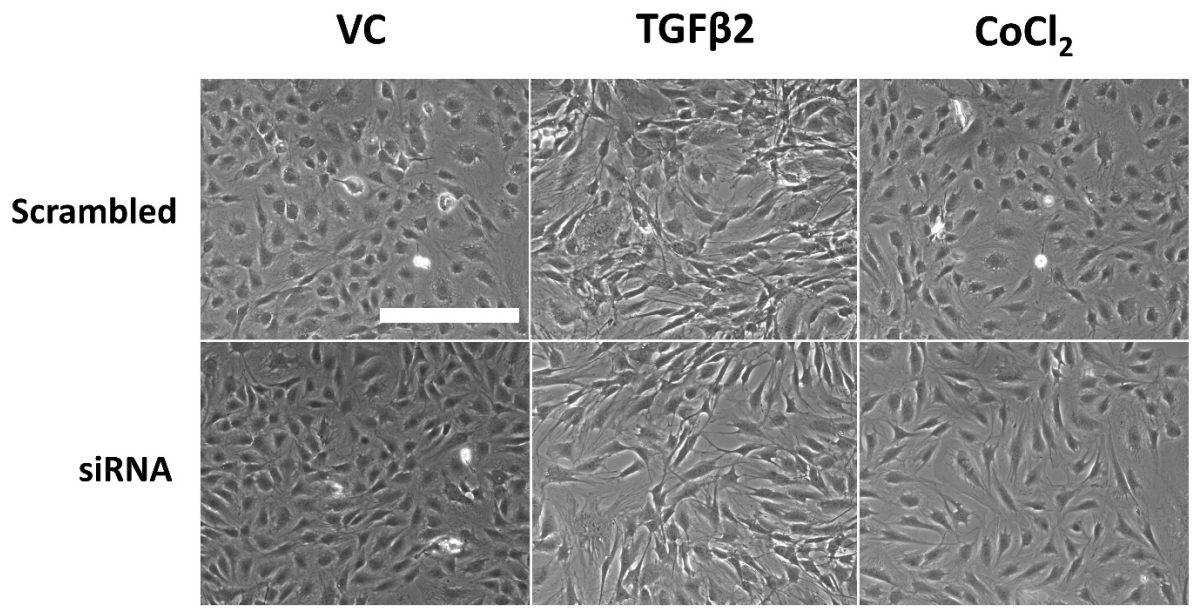

Supplemental 5. Phase-contrast images of C3H10T1/2 MSCs with siRNA knockdown and CoCl2 activation of HIF-1α. Representative phase-contrast images (10x) showing cell morphology with siRNA knockdown (siRNA) or scrambled control construct (Scrambled). Cells were further treated with either sterile water as the vehicle control (VC), TGFβ2, or $CoCl_2$ to chemically activate HIF-1α. Cells were cultured for 1 d, with early TGFβ2-associated morphological changes becoming apparent. Scale bar = 400 μm.

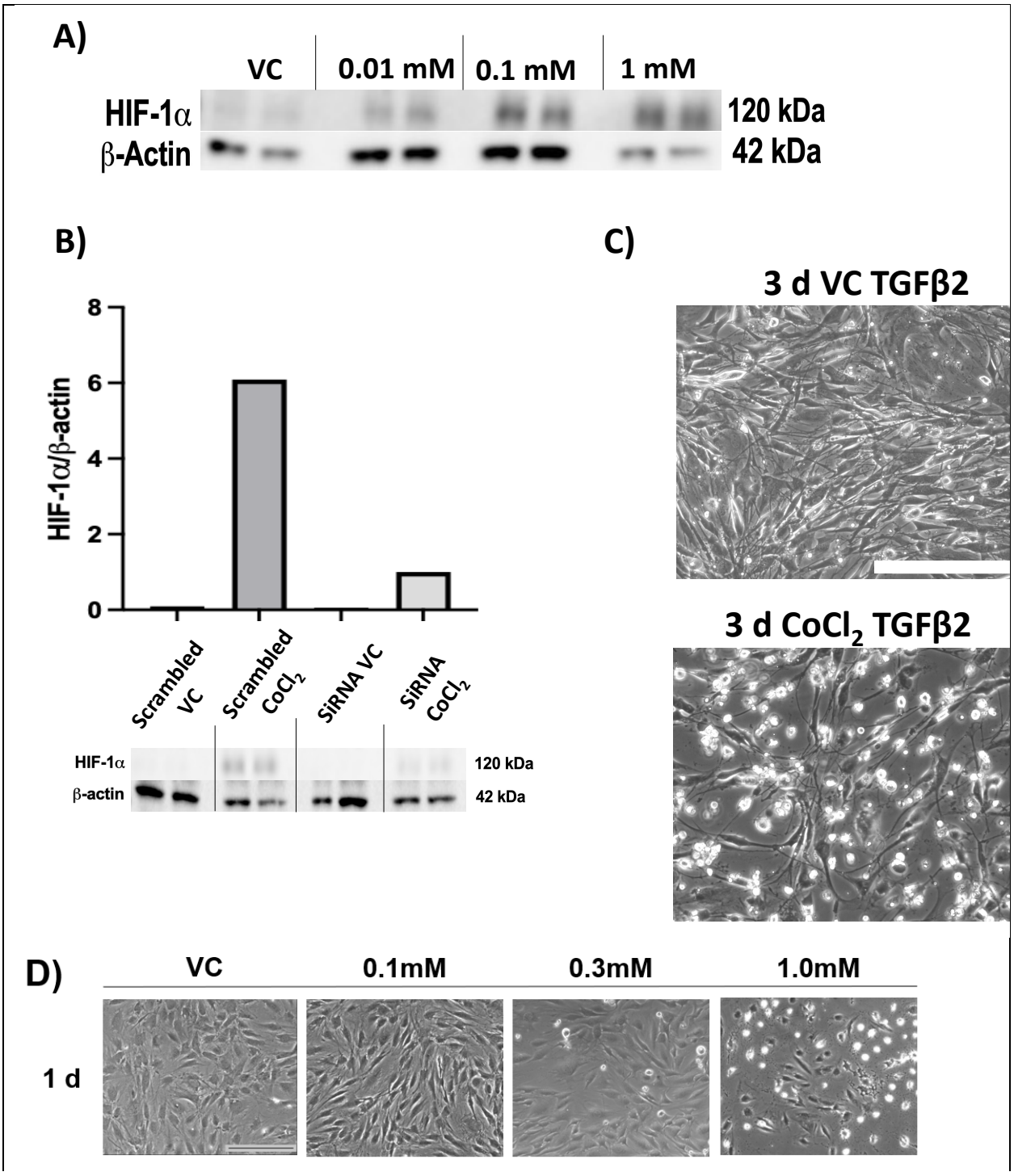
A)
VC
0.01 mM
0.1 mM
1 mM
HIF-1α
β-Actin
120 kDa
42 kDa
B)
HIF-1α/β-actin
8
6
4
2
0
Scrambled VC
Scrambled CoCl2
SiRNA VC
SiRNA CoCl2
HIF-1α
β-actin
120 kDa
42 kDa
C)
3 d VC TGFβ2
3 d CoCl2 TGFβ2
D)
VC
0.1mM
0.3mM
1.0mM
1 d

Supplemental 6. siRNA knockdown and activation of HIF-1α with Cobalt Chloride ($CoCl_2$). **A)** $CoCl_2$ concentrations of 0.01, 0.1, and 1mM were initially evaluated for HIF-1α activation. A 0.1 mM concentration of $CoCl_2$ was effective at activating HIF-1α at 1 d, while also maintaining cell viability. **B)** HIF-1α knockdown via siRNA was assessed with $CoCl_2$ treatment and a vehicle control (VC) and scrambled construct (Scrambled). The siRNA knockdown reduced HIF-1α in the presence of $CoCl_2$. **C)**. $CoCl_2$ treatment for extended timepoints (>3 d) resulted in decreased cell viability (shown here with representative phase-contrast images). Scale bar = 400 μm. **D)** A variety of $CoCl_2$ concentrations were tested to determine the highest concentration possible to use without affecting cell viability. A concentration of 0.1 mM $CoCl_2$ treatment was found to be effective without inducing noticeable cell death at a 1-day timepoint. Scale bar = 400 μm.

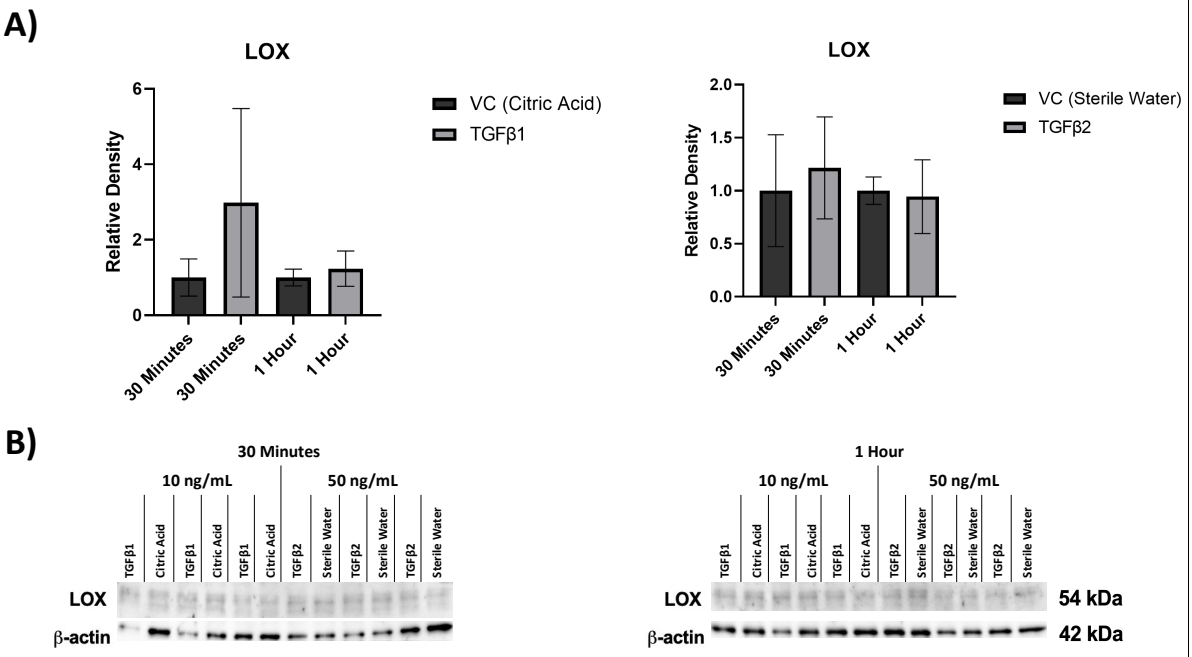

Supplemental 7. TGFβ1 and TGFβ2 do not impact LOX production by C3H10T1/2 MSCs at early timepoints. **A)** Western blot densitometry for LOX for treatments of 10 ng/mL TGFβ1 or 50 ng/mL TGFβ2 (n=3/treatment, n=3/timepoint), and **B)** representative LOX (54 kDa) and β-actin (42 kDa) bands. Both TGFβ1 and TGFβ2 showed no significant change in LOX levels at 30 minutes or 1 hour. $p > 0.05$